Electronic structure of small copper oxide clusters: From Cu_2O to Cu_2O_4

Lai-Sheng Wang,* Hongbin Wu, and Sunil R. Desai
Department of Physics, Washington State University, Richland, Washington 99352
and Environmental Molecular Sciences Laboratory, Pacific Northwest Laboratory, MS K2-14, P.O. Box 999, Richland, Washington 99352

Liang Lou
Rice Quantum Institute and Departments of Chemistry and Physics, Rice University, Houston, Texas 77251
(Received 25 October 1995; revised manuscript received 21 November 1995)

We study the electronic structure of copper oxide clusters, Cu_2O_x ($x=1-4$), using anion photoelectron spectroscopy and density-functional calculations. The experiment is used to successfully guide a computational search for the cluster geometries. The predicted electron affinities at the obtained cluster structures reproduce exactly the trend observed experimentally. The definitive determination of the cluster structures enables a detailed analysis of the chemical bonding and electronic structure involving Cu atoms in different oxidation states exhibited by these clusters.

The study of atomic clusters is attractive because they offer the opportunity to examine how atomic or molecular properties evolve into that of the condensed phases, and represent interesting molecular species that often exhibit remarkable physical and chemical properties.[1] Their finite sizes make more accurate *ab initio* calculations possible, and provide ideal models to study local effects taking place on surfaces and in the bulk.[2] Despite considerable experimental advances in the last decade, there is yet no direct experimental method to determine the structures of free clusters. On the other hand, theoretical approaches that have been proven highly accurate for determining molecular structures can be used to obtain definitive cluster structural information in combination with experimental studies.[3–5] In particular, it has recently been shown that cluster structures can be obtained by comparing first-principles simulations with photoelectron spectroscopy of size-selected anion clusters.[5] Metal oxide clusters, at which few efforts have been directed,[6] are interesting due to the scientific and technological importance of oxide materials.[7] We are interested in understanding the electronic and geometric structures of copper oxide clusters and their chemical bonding properties. These clusters are particularly important because they may provide better model systems to understand the electronic structure of copper oxide materials relevant to the copper oxide superconductors.[7]

In this paper, we present a combined study of a series of copper oxide clusters, Cu_2O_x ($x=1-4$), using anion photoelectron spectroscopy (PES) and *ab initio* density-functional theory (DFT) calculations. Detailed electronic and vibrational information of these clusters is revealed from the PES experiment. We determine the cluster structures by comparing the experimental observable, such as the electron affinities and the vibrational frequencies, with the DFT calculations. We found that from Cu_2O to Cu_2O_3 each O atom bridge bonds to the Cu_2 dimer, accompanied by a systematic increase of the electron affinity. Cu_2O_4 at which there is no electron affinity increase, assumes a hexagonal planner structure with two O_2 units bridge bonded to the Cu_2 dimer. The copper atoms in these systems are sequentially oxidized from an oxidation state of $+1$ in Cu_2O to $+3$ in Cu_2O_3, at which the oxidation is saturated, leading to two O-O units in Cu_2O_4. This observation is consistent with the known oxidation states for copper in the bulk oxides that can have a range of compositions due to the variable oxidation states of copper,[7] and suggests that the cluster studies can provide relevant information to the understanding of the bulk.

The $Cu_2O_x^-$ species are produced using a laser vaporization cluster beam apparatus, equipped with a magnetic bottle time-of-flight (TOF) photoelectron analyzer.[8] The details of the apparatus have been published.[9,10] Briefly, a copper target is vaporized into a helium carrier gas containing a small amount of O_2 (0.1%). The oxide clusters produced undergo a supersonic expansion to form a collimated cluster beam, from which the negative clusters are extracted perpendicularly into a TOF mass analyzer. The clusters of interest are selected by a mass gate and then decelerated before interaction with a detachment laser beam. Several detachment energies (532, 355, and 266 nm) are used to allow good energy resolution for the low-lying excited states since the resolution of the TOF electron analyzer is better with lower-energy electrons. All PES spectra are calibrated with the known spectrum of Cu^- and smoothed with either a 3- or 5-meV (for the 266-nm spectra) window function. We obtain the presented binding-energy spectra by subtracting the measured electron kinetic-energy distributions from the respective detachment photon energies.

Figure 1 shows the PES spectra of Cu_2O_x ($x=1-4$) with well-resolved ground states (labeled X) and low-lying excited-state features (labeled A, B, C, and so on in ascending order). The weak signals seen at the low binding-energy side in the spectra of Cu_2O_{2-4} are most likely due to thermal excitations in the anions and isomers with weakly bound O_2 as observed for CuO_2.[10] The measured energies of all the states are listed in Table I. The adiabatic electron affinity (EA) of the neutral clusters, derived from the ground-state feature, clearly shows a stepwise increase with x up to $x=3$ and levels off at $x=4$. Extensive vibrational structures are resolved for the X and A bands of Cu_2O_2. However, the spectra of all other clusters show relatively sharp electronic

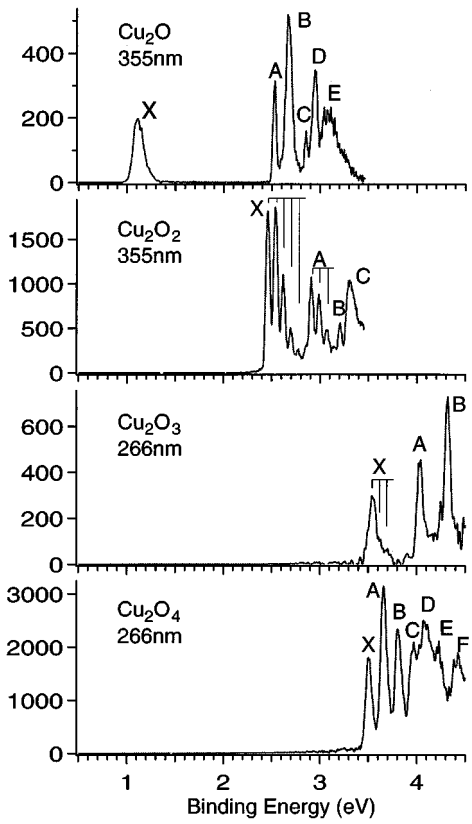

FIG. 1. Photoelectron spectra of $Cu_2O_x^-$ ($x=1-4$). The ground states of the neutral clusters are labeled "*X*," and their low-lying electronic states are labeled with the alphabet. The vibrational structures for the *X* and *A* bands of Cu_2O_2 and the *X* band of Cu_2O_3 are also indicated.

transitions with little vibrational excitation, indicating there is little geometry change from the anions to the neutrals. Discernible vibrational structures can be seen for the *X* band of Cu_2O_3 and the *E* band of Cu_2O. The peak width of the *X* band of Cu_2O indicates that there is vibrational excitation. But it could not be resolved even with a 25-meV (200-cm^{-1}) resolution when the 532-nm detachment light was used. The obtained vibrational frequencies are also listed in Table I.

The PES spectra (Fig. 1) contain a wealth of electronic structure information for the clusters. The Cu_2O spectrum shows a large gap between the *X* and *A* bands, representing the energy gap between the lowest unoccupied molecular orbital (LUMO) and the highest occupied molecular orbital (HOMO) of Cu_2O. The presence of the large HOMO-LUMO gap suggests neutral Cu_2O is an electronically closed shell. Similarities in both spectral features and intensity ratio are seen between the *A* and *C* bands, and between the *B* and *D* bands. These suggest that the origins of these bands should be due to two triplet-singlet pair states, arising from removing either a spin-down or spin-up electron from the inner filled orbitals just below the highest singly occupied orbital of Cu_2O^-. The details of the electronic structures and chemical bonding of the cluster series are better understood through the DFT calculations.

The fully optimized equilibrium structures of the Cu_2O_x ($x=1-4$) clusters are shown in Fig. 2, including geometric

TABLE I. Observed electronic states and vibrational frequencies of Cu_2O_x ($x=1-4$) clusters and predicted electron affinities and ground-state vibrational frequencies.

	BE[a] (eV)	ν (exp)[b] (cm^{-1})	EA[c] (eV)	ν (theor)[d] (cm^{-1})
Cu_2O[e]				
X	1.10	<200	1.10	$\nu_1=681$[f]
A	2.53			$\nu_2=156$
B	2.66			$\nu_3=586$
C	2.85			
D	2.95			
Cu_2O_2				
X	2.46	630 (30)	2.12	182 302 466
A	2.91	650 (30)		493 653 718[f]
B	3.12			
C	3.30			
Cu_2O_3				
X	3.54	(640)	3.03	259 259 318
A	4.02			321 321 351
B	4.32			608 608 678[f]
Cu_2O_4[e]				
X	3.50		2.94	119 222 244
A	3.66			267 277 354
B	3.80			533 612 612
C	3.95			647 912 985[f]

[a]Measured electron binding energy (uncertainty: ±0.03 eV). The binding energy (BE) of the *X* ground state yields the measured adiabatic electron affinity.

[b]Measured symmetric stretching vibrational frequencies for the given states (see text). Relative peak positions can be determined more accurately.

[c]Calculated adiabatic electron affinities in eV.

[d]Calculated vibrational frequencies for the ground-state cluster structures shown in Fig. 2.

[e]More highly excited states are not listed due to their broad and overlapping nature.

[f]Totally symmetric vibrational modes.

parameters and atomic charges from Mulliken population analyses. The local-spin-density (LSD) correlation potential of Vocko, Wilk, and Nusair is used in determining the cluster geometries.[11] The computational method utilizes three-dimensional numerical integration and a multiple expansion for the electrostatic potentials. The basis functions used are numerical solutions of the involved atoms and their proper ionic states. For Cu, a double-zeta plus single-polarization basis is used, while for oxygen a similar type of basis augmented with a pair of *s* and *p* functions is used.[12] Test calculations on Cu_2 and CuO diatomics are summarized in Table II, showing very good agreement with experiments.[13,14] The gradient correction, applied perturbatively,[12,15] significantly reduces the atomization energy values overestimated by the LSD, but does not change the calculated electron affinity as much because it affects both the anion and the neutral similarly. The overestimate of the vibrational frequency for CuO is largely due to the anharmonicity in the CuO potential well.

The ground states of Cu_2O and Cu_2O_2 are found to be a C_{2v} triangle and a D_{2h} rhombus, respectively. For Cu_2O_3,

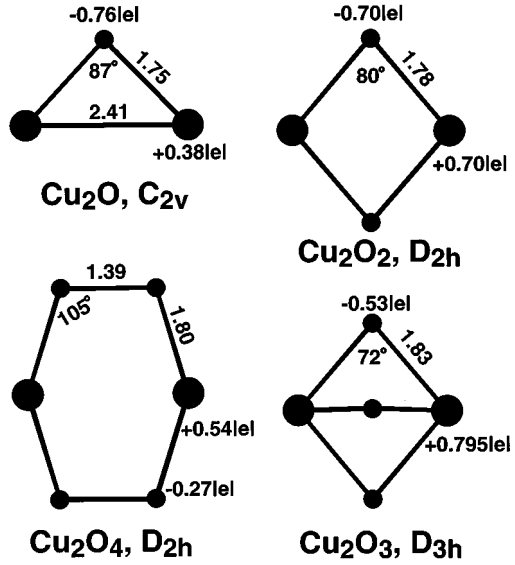

FIG. 2. The optimized structures and Mulliken charge distributions from density-functional theory calculations for Cu_2O_x ($x=1$–4).

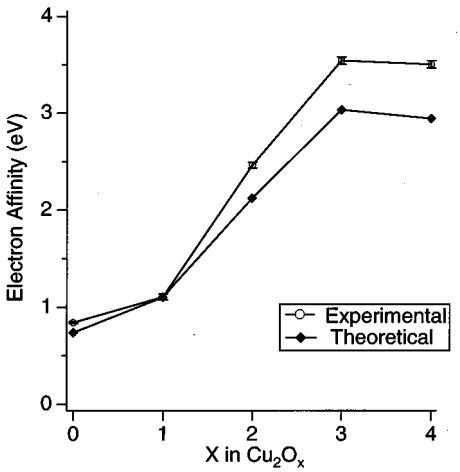

FIG. 3. Comparison of the calculated adiabatic electron affinities to that from the experiments. The experimental value for Cu_2 is from Ref. 13.

two isomers with close energies are found: a D_{3h} bipyramid (Fig. 2) and a C_{2v} bent structure with an O-Cu-O-Cu-O atomic arrangement. The C_{2v} structure is slightly favored by about 0.5 eV, but it yields an EA about 1 eV higher than the experimental value. As will be seen below, the D_{3h} structure gives an EA that is in better agreement with the experiment and is responsible for the observed PES spectrum. A D_{2h} hexagonal ring with two O-O bonds is found to be the most stable structure for Cu_2O_4.

The calculated EA values (Table I) increase stepwise with x and level off at $x=4$, following closely the trend of the experimental values (Fig. 3). Note that for Cu_2O_3, the D_{3h} isomer is chosen for comparison. The calculated EA for the C_{2v} bent isomer of Cu_2O_3 (4.4 eV) is out of the scale of Fig. 3. From the overall accuracy of the calculated EA, we suspect that the C_{2v} isomer may have a real EA value larger than the photon energy (4.66 eV) used in the experiment, and could not have been observed even if it was present in the cluster beam. This atomic arrangement is optimal for the localization of charges around the O centers, leading to the extremely high EA. The four clusters (Fig. 2) are all found to have closed-shell electronic structure in the neutral ground states. The calculated HOMO-LUMO gap for Cu_2O is 1.2 eV, and in the range of 0.2–0.6 eV for Cu_2O_{2-4}, in good agreement with the experiments. The smaller gaps for the larger clusters imply that stronger correlation effects may be present, leading to the deteriorated agreement between the calculated EA values and the experiments for the larger clusters. On the other hand, the large HOMO-LUMO gap in Cu_2O is responsible for the nearly perfect agreement between its calculated EA and the measured value. The same is true for Cu_2, for which excellent agreement is obtained between the current calculation and the measured value.[13]

TABLE II. Density-functional calculations for Cu_2 and CuO and their anions compared to experimental measurements (in parentheses). The experimental spectroscopic values are from Refs. 13 and 14 for the copper dimer and monoxide, respectively.

	Cu_2	Cu_2^-	CuO	CuO^-
E(LSD)[a] (eV)	2.46	3.16	4.01	5.73
E(PB86)[b] (eV)	1.89 (2.03)	2.57	3.21 (2.75)	4.82
EA (eV)	0.74 (0.84)		1.68 (1.78)	
bond length (Å)	2.19 (2.22)	2.31 (2.34)	1.69 (1.73)	1.67 (1.67)
ν (cm^{-1})	285 (265)	216 (210)	735 (631)	773 (739)

[a]Atomization energy at the local-spin-density approximation level.
[b]Atomization energy after gradient correction is applied. The experimental dissociation energy of the neutral is in the parentheses.

Vibrational structures resolved in the PES experiments provide important information about the cluster structures. The calculated vibrational frequencies (Table I) for the Cu_2O_x clusters agree well with the observed ones for $x=1$–3, where vibrational information is available. The unresolved vibrational structure in the X band of Cu_2O largely involves the Cu-Cu stretching vibration, since the LUMO of Cu_2O is mainly of Cu $4s\sigma$ bonding character. The experimental estimate of the upper bound of this mode is 200 cm^{-1}, which is consistent with the calculation. The 630-cm^{-1} vibrational frequency resolved for the ground state of Cu_2O_2 is due to the totally symmetric mode because only totally symmetric vibrational modes are expected to be active in PES experiments. The calculated frequency for this mode is 724 cm^{-1}, in reasonable agreement with the experiment. The estimated 640-cm^{-1} frequency for the ground state of Cu_2O_3 also compares favorably to the totally symmetric mode of 678 cm^{-1} from the calculation. As mentioned above, highly accurate vibrational frequencies are difficult to obtain due to the neglect of the anharmonicity in the calculations.

Several interesting trends can be observed in the evolution

of the atomic structures and chemical bonding in these clusters. First, the Cu-O bond length steadily increases as more oxygens ($x=1-3$) are added to the Cu_2 dimer, all occupying bridge positions. The increase in Cu-O bond length is accompanied by a decrease of atomic charges at the respective O sites. The atomic charge distribution suggests significant ionic bonding between Cu-O. Second, the Cu-O-Cu bond angle decreases from near 90° in Cu_2O to about 70° in Cu_2O_3. The smaller bond angle allows the bridge-bonded oxygens to separate further away from each other, and induces a shortening of the Cu-Cu distance. Third, the oxidation state of the copper atoms in the clusters, as formally indicated by the number of directly connected oxygens, raises from $+1$ in Cu_2O to $+3$ in Cu_2O_3, and then drops to $+2$ in Cu_2O_4. The lowering of the oxidation state for Cu_2O_4 is caused by the formation of two O-O bonds.

Therefore, we are seeing an interesting trend of sequential oxidation and oxidation saturation. The Cu atoms are oxidized formally from $+1$ to $+3$ from Cu_2O to Cu_2O_3 saturating at Cu_2O_4, where the further increase in the oxygen content does not lead to further oxidation, and the coordination of copper is reduced to 2. This agrees with the known chemistry of copper, whose common oxidation states are $+1$ and $+2$. The $+3$ oxidation state is rare, and is known to occur in the copper oxide superconductors and other materials.[16] The $+4$ oxidation state is extremely rare, and occurs only in certain compounds of fluorine,[16] the most oxidizing chemical element. Therefore, it is not surprising that the $+4$ oxidation state is not realized in Cu_2O_4, which is close to a peroxide. The sequential oxidation has a strong effect on the stability of the extra charge as manifested by the large stepwise EA increase from Cu_2O to Cu_2O_3, caused by the increasing charge depletion on the Cu sites.

The Cu-O bond in the Cu_2O_x clusters is complicated, involving both ionic and covalent characters. The best case for illustrating the polarized covalent bonding nature between Cu-O is the Cu_2O triatomic, that has a triangular structure with a nearly perfect Cu-O-Cu bond angle for the O $2p$ bonding. It is seen clearly from Fig. 2 that there is a large charge transfer from Cu to O. Further analysis, based on the single-particle density matrix and in terms of molecular orbitals, shows that the charge transfer is mainly from the Cu $4s$ shell to the O $2p$ shell. The occupation of the O $2s$ shell changes very little ($<0.1|e|$). On the Cu atoms, the $4s$ electron is partially promoted to the $4p$ orbitals; the sp hybrids thus formed are spatially more oriented than the spherical $4s$ orbitals for optimal overlaps with the O $2p$. The Cu $3d$ orbitals also interact with the O $2p$, but the net contribution to the Cu-O bonding is negligible because of the almost exact cancellation between the bonding and antibonding components. The Cu-Cu interactions in the Cu_2O_x ($x=1-4$) clusters are essentially electrostatic. The covalent interaction is found to be negligible due to the cancellation between the bonding and antibonding overlap contributions. Therefore, the bonding in the Cu_2O_x clusters is dominated by the strong polarized covalent interactions between Cu-O and the intramolecular O (O_2) Coulomb repulsion.

Support for this research from the National Science Foundation is gratefully acknowledged. The computation was partially performed on the Intel Touchstone Delta supercomputer system. The experimental work was performed at Pacific Northwest Laboratory, a multiprogram national laboratory operated for the U.S. Department of Energy by Battelle Memorial Institute under Contract No. DE-AC06-76RLO 1830.

*Author to whom correspondence should be addressed.

[1] See, for example, *Physics and Chemistry of Finite Systems: From Clusters to Crystals*, edited by P. Jena, S. N. Khanna, and B. K. Rao (Kluwer Academic, Boston, 1992), Vols. I and II.

[2] D. M. Rayner *et al.*, Phys. Rev. Lett. **74**, 2070 (1995).

[3] P. Dugourd *et al.*, Phys. Rev. Lett. **67**, 2638 (1991); E. C. Honea *et al.*, Nature **366**, 42 (1993).

[4] J. Fan, L. Lou, and L. S. Wang, J. Chem. Phys. **102**, 2701 (1995); J. B. Nicholas *et al.*, *ibid*. **102**, 8277 (1995); J. Fan *et al.*, J. Am. Chem. Soc. **117**, 5417 (1995).

[5] N. Bingggeli and J. R. Chelikowsky, Phys. Rev. Lett. **75**, 493 (1995); C. Massobrio, A. Pasquarello, and R. Car, *ibid*. **75**, 2104 (1995).

[6] G. C. Nieman *et al.*, High Temp. Sci. **22**, 115 (1986); J. R. Gord, R. J. Bemish, and B. S. Freiser, Int. J. Mass Spectrom. Ion Phys. **102**, 115 (1990); P. J. Ziemann and A. W. Castleman, J. Chem. Phys. **94**, 718 (1991).

[7] V. E. Henrich and P. A. Cox, *The Surface Science of Metal Oxides* (Cambridge University Press, New York, 1994).

[8] P. Kruit and F. H. Read, J. Phys. E **16**, 313 (1983); O. Cheshnovsky *et al.*, Rev. Sci. Instrum. **58**, 2131 (1987).

[9] L. S. Wang, H. S. Cheng, and J. Fan, J. Chem. Phys. **102**, 9480 (1995).

[10] H. Wu, S. R. Desai, and L. S. Wang, J. Chem. Phys. **103**, 4363 1995.

[11] A. D. Becke, J. Chem. Phys. **88**, 2547 (1988); B. Delley, *ibid*. **92**, 508 (1990); S. H. Vocko, L. Wilk, and M. Nusair, Can. J. Phys. **58**, 1200 (1980).

[12] L. Lou, P. Nordlander, and B. Hellsing, Surf. Sci. **320**, 320 (1994).

[13] D. G. Leopold, J. Ho, and W. C. Lineberger, J. Chem. Phys. **86**, 1715 (1987).

[14] M. L. Polak *et al.*, J. Phys. Chem. **95**, 3460 (1991).

[15] A. D. Becke, Phys. Rev. A **38**, 3098 (1988); C. Lee, W. Yang, and R. G. Par, Phys. Rev. B **37**, 785 (1988).

[16] A. F. Well, *Structural Inorganic Chemistry*, 5th ed. (Oxford University Press, New York, 1987).